Title

Chronic alcohol exposure alters action control via hyperactive premotor corticostriatal activity

Journal

Cell Reports, 42(7)

ISSN

2639-1856

Authors

Schreiner, Drew C

Wright, Andrew

Baltz, Emily T

et al.

Publication Date

2023-07-01

DOI

10.1016/j.celrep.2023.112675

Peer reviewed

HHS Public Access

Author manuscript

Cell Rep. Author manuscript; available in PMC 2023 August 31.

Published in final edited form as:

Cell Rep. 2023 July 25; 42(7): 112675. doi:10.1016/j.celrep.2023.112675.

Chronic alcohol exposure alters action control via hyperactive premotor corticostriatal activity

Drew C. Schreiner[1], **Andrew Wright**[1], **Emily T. Baltz**[2], **Tianyu Wang**[1], **Christian Cazares**[2], **Christina M. Gremel**[1,2,3,*]

[1]Department of Psychology, University of California San Diego, La Jolla, CA 92093, USA

[2]The Neurosciences Graduate Program, University of California San Diego, La Jolla, CA 92093, USA

[3]Lead contact

SUMMARY

Alcohol use disorder (AUD) alters decision-making control over actions, but disruptions to the responsible neural circuit mechanisms are unclear. Premotor corticostriatal circuits are implicated in balancing goal-directed and habitual control over actions and show disruption in disorders with compulsive, inflexible behaviors, including AUD. However, whether there is a causal link between disrupted premotor activity and altered action control is unknown. Here, we find that mice chronically exposed to alcohol (chronic intermittent ethanol [CIE]) showed impaired ability to use recent action information to guide subsequent actions. Prior CIE exposure resulted in aberrant increases in the calcium activity of premotor cortex (M2) neurons that project to the dorsal medial striatum (M2-DMS) during action control. Chemogenetic reduction of this CIE-induced hyperactivity in M2-DMS neurons rescued goal-directed action control. This suggests a direct, causal relationship between chronic alcohol disruption to premotor circuits and decision-making strategy and provides mechanistic support for targeting activity of human premotor regions as a potential treatment in AUD.

Graphical abstract

*Correspondence: cgremel@ucsd.edu.

AUTHOR CONTRIBUTIONS

Conceptualization, D.C.S. and C.M.G.; formal analysis, D.C.S. and C.C.; funding acquisition, D.C.S. and C.M.G.; investigation, D.C.S., A.W., E.T.B., T.W., and C.M.G.; methodology, D.C.S. and C.M.G.; visualization, D.C.S. and C.M.G.; writing – original draft, D.C.S., A.W., and C.M.G.; writing – review & editing, D.C.S., C.C., E.T.B., and C.M.G.; supervision, C.M.G.; project administration, C.M.G.

SUPPLEMENTAL INFORMATION

Supplemental information can be found online at https://doi.org/10.1016/j.celrep.2023.112675.

DECLARATION OF INTERESTS

The authors declare no competing interests.

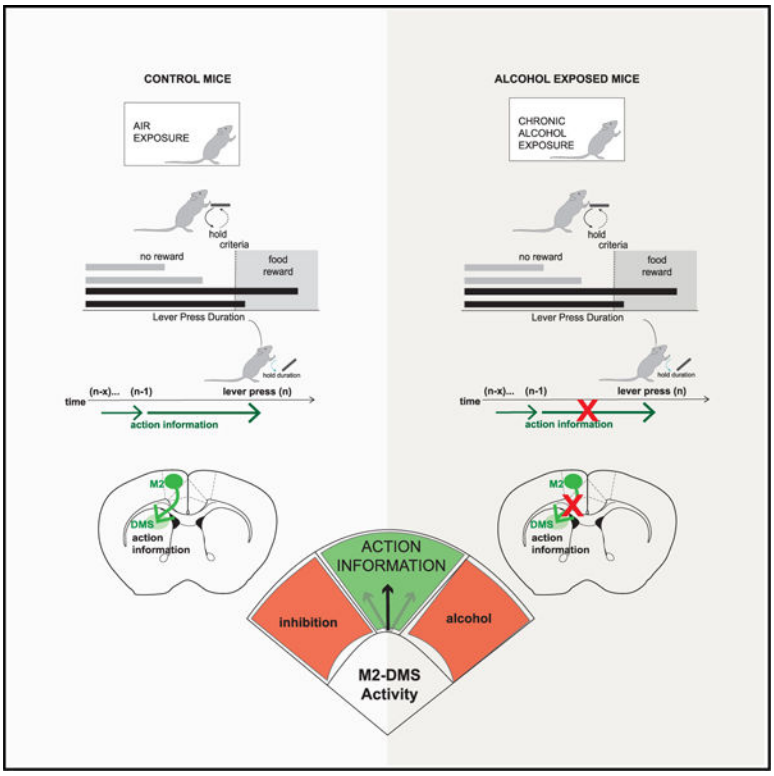

In brief

Appropriate action control relies on learning from recent experiences. Using a rodent model, Schreiner et al. find evidence that chronic alcohol exposure disrupts action control by inducing aberrant hyperactivity in premotor corticostriatal circuits. These findings support the targeting of premotor cortex activity for therapeutic treatment in alcohol use disorder.

INTRODUCTION

Alcohol use disorder (AUD) is associated with alterations to decision-making, including goal-directed strategies employed to control one's actions.[1–6] Goal-directed control allows one to use information about the value of the consequence produced by the action (do I want it?) as well as knowledge about what action is needed to achieve that consequence (how do I get it?) to guide behavior. Loss of goal-directed control can result in what is commonly termed habits.[7,8] AUD-related alterations to decision-making may contribute to daily dysfunction, continued alcohol abuse, and relapse,[9–11] suggesting that targeting restoration of action control has treatment potential.[12] Pre-clinical work has found AUD-related alterations to regions important for goal-directed action control, including regions of the prefrontal cortex,[13–18] and cortical output into the striatum.[17–24] However, the specific circuits and mechanisms disrupted in AUD responsible for altering action control strategies are not clear. As novel approaches are being explored in the treatment of drug dependence, including repetitive transcranial magnetic stimulation (rTMS) targeting of the dorsal cortex, it is essential to identify the circuit-specific mechanisms involved.

The pre-supplementary/supplementary motor areas (pre-SMA/SMA) present a potential but understudied treatment candidate. Pre-SMA/SMA send extensive projections into the dorsal striatum, are disrupted in AUD,[2,3,6,25] and are involved in supporting flexible action control.[26–28] In a rhesus macaque model, activity of pre-SMA neurons was increased during goal-directed control versus habits.[29] Further, electrical stimulation led monkeys to switch from habitual to goal-directed action control,[29] prompting the hypotheses that pre-SMA activity was recruited for suppressing habits and/or supporting goal-directed action control.

Indeed, altered activity of pre-SMA/SMA circuits has been implicated in disease states with disordered action control, including AUD.[30–32] Abstinent individuals with AUD show impaired response inhibition and reduced SMA volume.[3] However, correlative studies have been less clear, as task designs have varied. On one hand, SMA activity positively correlated with AUD severity, with more severe symptoms associated with greater recruitment of SMA activity during delay discounting.[2] On the other hand, another study reported a hypoactive SMA during performance of a response inhibition task.[6] Despite these discrepant findings, these studies do suggest that pre-SMA/SMA function may be altered in AUD during action control. However, crucially missing is a causal link between AUD-related effects on pre-SMA/SMA function and altered action control.

The pre-SMA/SMA's homolog in rodents, the premotor cortex (M2; also known as secondary motor cortex, bregma: +1 mm anterior),[33] has been shown to be important for goal-directed and experience-based action control.[34–41] M2 sends broad and dense projections innervating the striatum, including the dorsal medial striatum (M2-DMS; DMS, akin to the primate caudate nucleus) as well as the dorsal lateral striatum.[42–44] We recently showed in mice that M2 and M2-DMS projection neuron activity represents both current and prior action-related information.[40] M2 and M2-DMS projection activity was functionally necessary for action control; lesions and behavior-dependent optogenetic inhibition of M2-DMS projection activity prevented mice from using information gleaned from the prior action to guide their next action.[40] These findings support the hypothesis that M2-DMS contributes to the use of recent action performance to guide goal-directed action control,[29] thus raising the possibility that its disruption could contribute to disease states with disordered action control, including AUD. Indeed, prior works have shown that this M2-DMS projection is potentiated in a rodent model of obsessive compulsive disorder and is involved in working memory deficits in a rodent model of Parkinson's disease.[45,46]

However, limited mechanistic examination of rodent M2 has been done in the context of alcohol, AUD-related, or substance use disorder effects, and even less on how specific M2 projections may be involved. Brain-wide scans in rodents revealed that acute alcohol increased cFos within M2[47] and that chronic alcohol increased M2 activity, as assessed via MRI.[48] This suggests that chronic alcohol exposure may induce long-lasting changes to the activity and function of M2, thereby altering its contribution to goal-directed action control. Here, we examined whether chronic alcohol induced long-lasting changes to the activity and function of M2 neurons with projections into the DMS. We used a model of chronic alcohol exposure and withdrawal in mice that increases withdrawal severity and ethanol consumption and disrupts goal-directed control.[1,17,49–54] In protracted withdrawal, we then

examined persistent chronic alcohol effects on M2-DMS projection neuron activity and their contribution to action control during decision-making.

RESULTS

Prior CIE impairs the use of recent experience to guide decision-making

Equal numbers of male/female (M/F) C57BL/6J mice were exposed to 4 weeks of chronic intermittent ethanol (CIE) exposure and withdrawal or air vapor control (Air) (Figure 1A)[1,17,49–54] and then underwent instrumental training during protracted withdrawal to reduce the effects of acute withdrawal on behavioral measures.[55] Of note, we employed an instrumental lever press task[40,52,56–59] that allowed for analysis of continuous action control in which one can quantify the influence of prior sequential (n – x back) lever presses on the current lever press. Prior work has shown that lever press behavior in this task is goal directed[40,52,58] and that prior CIE disrupts goal-directed control in this task, as indexed by reduced sensitivity to outcome devaluation procedures.[52] Importantly, in contrast to contingency degradation and outcome devaluation procedures, use of this task allows us to examine action control independent of changes to the relationship between an action and its associated reward or to changes in the reward itself.[60,61] In this task, mice learned to press and hold down a lever for at least a minimum duration in order to earn a food reward, with the duration requirement increasing from 800 to 1,600 ms across days (Figure 1A). There were no cues or trials, the behavior was self-paced, and reward was delivered only after mice released the lever (Figure 1B). Thus, mice were left to rely only on their prior experience to guide performance.

We first assessed acquisition behavior and found that Air and CIE mice similarly decreased the number of lever presses across days under both 800 and 1,600 ms duration training days (Figure 1C). Both groups also similarly decreased their rate of lever pressing, although on the very first day of duration training, CIE mice had increased response rates compared with Air mice (Figure 1D). Air and CIE mice earned similar numbers of rewards (Figure 1E). Although the task was not qualitatively easy for mice, performance efficiency increased similarly in Air and CIE mice across training days under each duration, reflecting task acquisition (Figure 1F). Further, the median lever press duration increased across sessions (Figure 1G), as well as within sessions (Figure 1H). Indeed, mice began to increase the median duration of their presses on the very first day of training. While Air mice had overall higher median durations than CIE mice across the first day of 800 ms training, median durations were similar by the last training day (Figure 1H). Further, all mice showed a significant rightward shift in their distribution of press durations after the duration criteria increased, with Air and CIE mice showing similar duration distributions on the final days of 800 and 1,600 ms training (Figure 1I). Collectively, these data show that Air and CIE mice were able to learn and perform this task at relatively similar levels, although CIE mice showed small differences in initial rates and durations of lever pressing. However, Air and CIE mice could be using different behavioral strategies to reach similar levels of performance.[17,18]

One possibility is that Air and CIE mice could rely on prior action experience to varying degrees (e.g., exploration versus exploitation[62]). For instance, CIE may result in mice

making sequential lever press durations that are more, or less, related to prior durations. To address this question, we built linear mixed effect (LME) models to predict the duration of each lever press (n) given the durations of prior lever presses (n – 1 through n – 10) (Figure 2A). The β coefficients of the individual n-back press covariates in our models reflect the degree to which mice used prior lever press durations to inform their subsequent pressing (higher values reflect stronger use of prior duration information). We found that Air mice relied on the durations of recently executed lever presses to inform their current press duration, with this contribution of prior action durations rapidly decaying across n-back presses (Figure 2B). The use of prior action information was not an artifact of random lever pressing; comparisons with order shuffled data (for each shuffled n-back comparison, we shuffled just the order of a particular lagged lever press [e.g., only n – 3] within a given mouse within a given day, thus controlling for the overall statistics of the press durations while shuffling only their serial order) showed that mice clearly used prior action information to guide pressing and did not randomly execute lever press durations (see STAR Methods for a detailed model explanation). CIE exposure attenuated this reliance on recent action information; relative to Air mice, the current lever press duration in CIE-exposed mice was less related to the duration of the immediately prior lever press (Figure 2B; see also Table S1). This was also true in an alternative LME model built with both groups together in the same model and Air/CIE indicator variables (n – 1 coefficient for the CIE group relative to Air = −0.056, $F_{1,50083} = 44.7$, p = 2.29e–11). Furthermore, LME models built using individual session data showed that only in Air mice was the magnitude of the n – 1 β coefficient positively correlated with rewarded performance (Figure 2C). That is, the more that Air mice used duration information from their recent lever press, the better they performed at the task. This relationship was not present in CIE mice (Figure 2D). Collectively, these results suggest that prior CIE impaired the ability of mice to use recent action contingency information to guide subsequent lever press durations for efficient performance, a hallmark of goal-directed action control.

Prior CIE induces hyperactive *in vivo* calcium activity of M2-DMS projection neurons and uncouples activity and behavior

To address if CIE affects M2-DMS activity, modulation, and function during behavior, we used a dual-virus cre-dependent strategy to express the fluorescent calcium indicator GCaMP6s only in M2-DMS projection neurons and implanted optical ferrules centered on M2 prior to CIE exposure (Figures 3A and S1A). We then recorded bulk population calcium activity of M2-DMS projection neurons in Air and CIE mice using *in vivo* fiber photometry during task performance. Peak analysis of the session-long calcium signal[63] showed that prior CIE led to a significant increase in overall calcium transients across sessions (Figures 3B and 3C). However, prior CIE did not disrupt the overall intrinsic excitability of M2-DMS projection neurons (Figure S2), suggesting that increased *in vivo* activity may arise from changes in transmission within M2.

Prior CIE may also lead to alterations in the recruitment and/or modulation of calcium activity during task performance. We aligned calcium activity to the onset, time-warped hold duration, and offset of lever pressing. We z scored and averaged the calcium activity across all trials for all mice relative to a baseline period (−15 to −5 s prior to press onset).

Permutation testing[64] showed that CIE led to increased calcium activity throughout the entire press-aligned window (Figure 3D). We replicated these results using mouse average calcium activity with two-way ANOVA-based comparisons (Figure 3E). As the baseline period may sometimes include previous lever presses, we also calculated calcium activity as delta fluorescence/fluorescence (DF/F) using a session-long mean, which yielded largely similar results, with only a few time points before press onset no longer significantly different between Air/CIE groups (e.g., from −5 to −4 s before a press; Figure S1B).

The increased calcium activity in both Air and CIE mice just after press offset (Figures 3D and 3E, right) may reflect altered reward-related processing, as it often encompasses the period of reward retrieval and consumption. Therefore, we segmented all lever presses based on whether they met (rewarded) or failed to meet (unrewarded) the duration criteria. In both Air and CIE mice, the increased calcium activity after press offset was selective for Met presses (Figure 3F, right). There were also Met/Fail differences in calcium activity both before press onset as well as during action execution itself (Figure 3F). M2-DMS activity is differentially modulated by press durations before, during, and after those lever presses occur, suggesting that M2-DMS activity may predict and relate to press durations, as has been previously reported.[40] Thus, activity associated with performance of the same action (i.e., onset of lever pressing and lever pressing itself) is differentially modulated depending on whether that lever press will eventually produce a reward. Further, the average difference between met/fail lever presses was larger in CIE mice than Air mice at all three time points (Figure 3G). This raises the hypothesis that CIE alters the relationship between endogenous M2-DMS activity and press duration. To directly investigate this, we trained a linear support vector machine (SVM) decoder to predict lever press duration using calcium activity data with 10 k-fold cross-validations. We found significant decoding accuracy (chance at 25%) of lever press duration from M2-DMS activity, with decoding accuracy significantly reduced in CIE mice relative to Air mice (Figure 3H). Additionally, we built LME models that predicted calcium activity before, during, or after a lever press using current and prior lever press durations (as well as prior activity covariates to control for autocorrelation in the calcium signal; Tables S2–S4). Overall, we saw that both current and prior press durations influenced M2-DMS calcium activity at all three event epochs: before, during, and after lever presses. Importantly, we also observed an Air/CIE difference after lever press offset, where a given n – 1 duration led to greater calcium activity in CIE mice relative to Air controls (Table S4). Collectively, these results suggest that CIE induced hyperactivity of M2-DMS projections neurons, which eroded the endogenous relationship between M2-DMS activity and behavioral output.

Chemogenetic inhibition of hyperactive M2-DMS rescues use of recent experience

CIE increased M2-DMS *in vivo* activity and reduced use of recent action experience, but it was unclear whether CIE-induced M2-DMS activity changes causally led to the observed deficit in action control. To examine this, we applied a chemogenetic approach to reduce M2-DMS activity in Air and CIE mice. We used a dual-viral vector strategy to target expression of the cre-dependent inhibitory chemogenetic receptor hM4Di (H4) or the cre-dependent fluorophore tdTomato as a control (Ctl) to M2-DMS projection neurons in both Air and CIE-exposed mice (Figures 4A and S3A), giving four groups of comparison

(Air Ctl, Air H4, CIE Ctl, and CIE H4). Of note, this approach targets M2 neurons with projections to the DMS, as well as additional downstream collaterals. All mice received the H4-agonist clozapine-N-oxide (CNO) 30 min prior to every lever hold-down session (90 min session) (Figure 4B). We verified that CNO application reduced the excitability of M2-DMS neurons only in H4-expressing mice via *ex vivo* slice electrophysiology (Figure S3B).

As in our other manipulations, there were few differences between groups in coarse measurements of behavior including total lever presses (Figure 4C), percentage of presses that met criteria at 800 ms duration criteria (Figure 4D), and lever press durations on the final training day (Figure 4E). However, there was an Air/CIE group difference in percentage of presses that met criteria during 1,600 ms training, but no Ctl/H4 difference, nor a significant interaction between these factors. Furthermore, there were no group differences in the rate of lever pressing, nor in the number or rate of met criteria lever presses (Figures S3C–S3E). Thus, neither CIE nor M2-DMS inhibition led to large, sustained changes in coarse behavior, but again, mice could reach largely similar levels of performance using different behavioral strategies.

We once more built LME models to determine if mice were using the duration from their prior lever press to inform their current press duration (Figures 4F and S3F; Table S5). We found a significant interaction between vapor exposure and H4/Ctl groups on the magnitude of the n – 1 β coefficient (no main effects). Post hoc comparisons showed a replication of our initial finding (Figure 2B), with CIE Ctl mice having a significantly smaller magnitude n – 1 β coefficient relative to Air Ctl mice. Further, H4 expression in Air mice led to a significantly reduced magnitude n – 1 β coefficient relative to that observed in Air Ctl mice, replicating prior findings that M2-DMS activity contributes to the use of prior lever press duration information.[40] In contrast, comparing CIE H4 mice with CIE Ctl mice (i.e., the treatment group), we found an increase in the magnitude of the n – 1 β coefficient in CIE H4 mice. Indeed, the n – 1 β coefficient magnitude in CIE H4 mice did not differ from that of Air Ctl animals. This result was replicated in an alternative LME model built with all groups together in the same model and group indicator variables (three-way interaction among n – 1 duration × Air/CIE group × Ctl/H4 group $F_{1,80577} = 71.8$, $p = 2.4e{-}17$). Thus, by reducing M2-DMS projection neuron activity in CIE mice, we restored the use of recently executed lever press durations to guide current action control.

DISCUSSION

Premotor corticostriatal regions in humans and rodents are thought to support goal-directed and experience-based action control,[28,34,40] and their disruption is linked to compulsive disorders.[30–32,46] While there have been reports of alterations to premotor circuits in AUD,[2,3,6,25] there has been a dearth of insights into the neural mechanisms and the behavioral consequences of such disruption. Here, we show that prior chronic alcohol exposure alters action control by reducing the use of recent action contingency information to guide decision-making. This was due to an alcohol-induced increase in the activity of M2 neurons with projections into the striatum, as reducing activity restored use of recent experience. Our findings reveal a novel circuit through which chronic alcohol can alter

goal-directed action control and support the targeting of pre-SMA/SMA to treat altered executive function in AUD.[65]

Substantial evidence suggests that AUD can alter decision-making, including goal-directed control over actions.[2–6,10,66–69] However, a host of different computational mechanisms support goal-directed decision-making.[5,61] By using a continuous task, we were able to show that one specific aspect—the use of recent action contingency information to guide behavior—was disrupted by chronic alcohol exposure and controlled by M2-DMS projection neurons. Our results have important implications for AUD: we saw a disruption in recent action information for a non-drug reward in protracted withdrawal and altered M2 circuit engagement during action control. This suggests long-lasting neuroadaptations in M2 circuits arising in response to chronic alcohol exposure and withdrawal, as evidenced in part by observed increases in calcium activity. These long-lasting changes may contribute to alterations in executive function observed in AUD, including impulsivity and impaired response inhibition,[2,3,6] as both require the use of recent experience with one's actions to adjust or stop behavior. Given this, investigations into specific mechanisms of disrupted transmission onto M2-DM2 neurons as well as M2 generally are clearly warranted.

In the present findings, impaired sensitivity to recent action information was causally tied to M2-DMS activity, replicating prior findings.[40] Importantly, our main finding of reduced reliance on recent action information following CIE exposure was replicated across experiments. This supports and extends previous correlative evidence in humans showing that AUD is associated with disruption to both premotor regions and reduced flexibility.[2,3,6] We report increases in M2-DMS activity following CIE, while prior studies of premotor and prefrontal cortex function in humans with AUD variously report increases and decreases in activity.[2,3,6,25] This highlights the need to examine activity in a nuanced manner in relation to the computations being performed as well as the populations performing such computations in order to understand the functional consequences. This is likely to be especially important for precise targeting of novel region-specific treatments.

To our knowledge, this is the first study investigating the function of M2 neurons with projections to the dorsal striatum in the context of chronic alcohol. M2 is a dominant source of inputs into the medial striatum, where terminal fields converge with a wide array of cortical inputs.[42,43] Hypotheses related to habitual control in AUD[12,70] have suggested that increased motor and sensory input into the dorsal striatum may contribute to habit-related phenotypes. The present findings provide some support for this: chronic alcohol induced hyperactivity of M2-DMS calcium activity *in vivo* during task performance and altered action control processes. However, we also found weaker decoding of current press durations from this increased activity, and chemogenetically inhibiting this increased activity restored the usual activity-duration relationship. One of the most intriguing findings of the present study was that both increases (from prior CIE exposure) and decreases (from chemogenetic inhibition) in M2-DMS activity led to similar behavioral alterations. While the present work did not examine whether *in vivo* hyperactivity translated into increased M2-DMS transmission, this does suggest that the potential increased activity from M2-DMS following CIE may not directly support the observed phenotype, since reduced drive also leads to a similar phenotype. Rather, it may depend upon which inputs are recruited and

the pattern of activity produced. This adds to a growing body of literature suggesting that the patterning of neural activity is decisive and that there is not a simple linear relationship between brain activity and behavioral output.[71]

How might prior chronic alcohol produce hyperactive M2-DMS? We did not find CIE-induced alterations in the intrinsic properties of M2 projection neurons (Figure S2), suggesting that changes in circuit transmission are likely responsible for the increased calcium activity observed. One interesting candidate is the orbitofrontal cortex, as it is affected by alcohol[72,73] and its projection to M2 is implicated in decision-making and exploiting known rules.[41,74] A further question is whether there are synapse-specific alterations of M2 projections onto dorsal striatum neurons.[17,18,75] However, we did not examine terminal activity, and thus whether chronic alcohol alters M2 recruitment of dorsal striatal circuitry for behavioral control remains to be investigated.

Limitations of the study

It is important to note that while we used a dual-viral approach to target M2 neurons with projections into the DMS, we are unable to exclude potential downstream changes in dorsal lateral regions of the striatum, as M2-DMS neurons have collaterals extending into the DLS as well as other downstream areas. In addition, while response levels on the first day of task acquisition in the chemogenetic experiments differed from the levels observed in our behavioral experiments (perhaps as a consequence of potential stress from pre-injections of CNO), response levels quickly became similar across groups with similar $n-1$ β coefficients across experiments. Lastly, while we did not observe a change in excitability of M2-DMS projection neurons (Figure S2), this does not rule out potential compensatory adjustments to excitability following chronic alcohol exposure. Additional experiments examining transmission onto M2-DMS are warranted.

Conclusion

The human homologs of M2—pre-SMA/SMA—are dorsally located and accessible to region-specific treatments such as rTMS. Indeed, such treatments have shown promise in reducing compulsivity and improving cognitive control in obsessive compulsive disorder.[30–32] These prior works demonstrate a pre-clinical to clinical translation for premotor circuits involved in psychiatric disease and suggest that pre-SMA/SMA may be fruitful therapeutic targets for the treatment of AUD in human patients.[65] Here, we provide pre-clinical evidence supporting this potential treatment avenue, as well as mechanistic insight into the involved behavioral and neural controllers of goal-directed action control that are altered by AUD.

STAR★METHODS

RESOURCE AVAILABILITY

Lead contact—Further information and requests for resources and reagents should be directed to and will be fulfilled by the lead contact, Christina M Gremel (cgremel@ucsd.edu).

Materials availability—This study did not generate any new reagents.

Data and code availability

- The data reported in this paper will be shared by the lead contact upon request.
- The code used to analyze the data from this study is available at: https://github.com/gremellab/Hold-Down-Behavior-GCAMP-Opto-analysis (https://doi.org/10.5281/Zenodo.7972046)
- Any additional information required to reanalyze the data reported in this paper is available from the lead contact upon request.

EXPERIMENTAL MODEL AND SUBJECT PARTICIPANT DETAILS

Male and female (M/F) C57BL/6J mice (>7 weeks/50 PND) (The Jackson Laboratory, Bar Harbor, ME) were used for all experiments. Experiments were not sufficiently powered to detect sex differences, and data were collapsed across sex. All procedures were conducted during the light period and mice had free access to water. Mice were housed 2–4 per cage on a 14:10 light:dark cycle. Mice were food restricted to 85–90% of their baseline weight 2 days prior to starting behavioral procedures, and fed daily 1–4 hours after training. Mice were counterbalanced for sex, cage (i.e., littermates), and vapor cohort (see below) for allocation to experimental groups. All experiments were approved by the University of California San Diego Institutional Animal Care and Use Committee and were carried out in accordance with the National Institutes of Health (NIH) 'Principles of Laboratory Care'.

METHOD DETAILS

Surgical procedures—Viral vectors were obtained from the UNC Viral Vector Core (Chapel Hill, NC) or Addgene (Watertown, MA). Mice were anesthetized with isoflurane (1–2%) and intracranial injections (100 nl/min) were targeted at a relative posterior portion of M2 (from Bregma: AP +1.0mm, L ±0.5mm and V −1.2mm, −1.4mm from the skull), and DMS (from Bregma: AP +1.0mm, L ±1.65mm and V −3.0mm, −3.2mm from the skull). Mice were given at least one week of recovery prior to the start of CIE procedures. After behavioral testing was completed, mice were euthanized and brains were extracted and fixed in 4% paraformaldehyde. Virus localization and spread was assessed in 100 um thick brain slices via fluorescent microscopy (Olympus MVX10, Shinjuku, Japan).

For M2-DMS calcium imaging, n = 8 Air and n = 8 CIE mice (4 M/F per group) were unilaterally injected with a virus expressing a cre-dependent GCaMP6s in M2 (pAAV.CAG.FLEX.GCaMP6s.WPRE.SV40 (Addgene: 100842): 2 injection depths, 200nl each), and a retrograde-capable virus[77] expressing cre recombinase (AAV5/Ef1a-Cre-WPRE) in DMS (2 injection depths: 250nl each). Animals were then implanted with an optical ferrule centered on M2. Inclusion required viral expression within M2 and ferrule placement within M2. Two Air mice were excluded due to poor viral expression (to give final n = 6 Air).

For chemogenetic inhibition of M2-DMS, control animals (n = 6 Air (4/2 M/F), n = 6 CIE (3/3 M/F) were injected with a virus expressing cre-dependent tdTomato in M2 (rAAV5/

Flex-tdTomato), while experimental animals (n = 9 Air, n = 8 CIE) were injected with a virus expressing a cre-dependent inhibitory chemogenetic receptor hM4Di (H4) in M2 (pAAV5-hSyn-DIO-hM4D(Gi)-mCherry) (150 nl each injection depth). Both groups were injected with a retrograde-capable virus[77] expressing cre recombinase in DMS (rAAV5/hSyn-GFP-Cre) (200 nl each injection depth). Inclusion in data analyses required expression of virus centered within M2, with minimal spread into surrounding areas. One Air H4 mouse, and one CIE H4 mouse were excluded due to off-target viral expression (final n = 8 Air H4 (4/4 M/F) and n = 7 CIE H4 (4/3 M/F)).

For whole cell physiology of M2-DMS projection neurons, mice were injected with a retrograde-capable virus[77] rAAV5/hSyn-GFP into DMS (200 nl).

Chronic intermittent ethanol procedures—Mice (>8 weeks of age) were exposed to chronic intermittent ethanol vapor (CIE) or Air.[17,49–53] As previously described,[17,18,52] mice were exposed to Air/CIE vapor for 16 hrs/day, for four consecutive days, and this procedure was repeated for 4 weeks. Ethanol was volatilized by bubbling air through a flask containing 95% ethanol at a rate of 2/3 L/min, delivered to the mice housed in Plexiglas containers (Plas Labs Inc.). No loading dose of ethanol or pyrazole pretreatment was administered to reduce confounding effects of 1) stress on behavior[78] and 2) pyrazole on neural activity.[50,79] Blood alcohol concentration was collected from sentinel animals, with a mean ± SEM of 27.9 ± 2.0mM, 128.54 ± 9.21 mg/dl. The number of cohorts of Vapor mice for the following experiments are; behavior only: 1 vapor cohort, for Photometry: 3 counterbalanced vapor cohorts, for slice physiology: 2 cohorts, and for M2-DMS DREADD inhibition: 1 vapor cohort.

Behavioral procedures—To examine CIE-effects that persist into protracted withdrawal,[55] five days post the final vapor exposure, mice began daily operant training in sound-attenuating boxes (Med-Associates, St Albans, VT) in which they pressed a lever (left or right of the food magazine, counterbalanced) for an outcome of regular ‘chow’ pellets (20 mg pellet per reinforcer, Bio-Serv formula F0071). Each training session commenced with an illumination of the house light and lever extension and ended after either 60 reinforcers were earned or 90 minutes had elapsed, with the lever retracting and the house light turning off.

On the first day, mice were trained to approach the food magazine to retrieve the pellet outcome (no lever present) on a random time (RT 120s) schedule, for a total of 60 minutes. Next, mice were trained on a continuous ratio schedule of reinforcement (CRF) across 3 days, where every lever press was reinforced, and the total possible number of reinforcers increased (CRF10, 30, and 60) across days.

Following CRF pretraining, the lever-press duration contingency was introduced, in which mice had to press and hold down the lever for at least a minimum duration in order to earn food reward (delivered immediately after press release). Importantly, there were no cues, no timeout period, nor any discrete trials; the lever was always available to mice, until the session was complete. Mice were trained at the >800ms criterion for 6 days, followed by at least 6 days of training at the >1,600ms criterion. Timestamps for lever press onset

and offset, headentry into the food magazine onset and offset, and reward delivery were recorded. From these timestamps, we calculated durations of lever presses and headentries (20ms resolution).

Fiber photometry—Animals received one additional day of CRF pretraining when they were first connected to 400 um optical fiber tethers with ferrule-to-ferrule connectivity. GCaMP6s was excited using a 470nm LED at < 70 mW/mm2 (Thorlabs, Newton, NJ), with an isosbestic control for motion artifact at 405 nm LED. GCaMP6s fluorescence emission was collected using a bifurcated fiber (Thorlabs, Newton, NJ) that allowed for simultaneous, independent recordings from two mice. The dual fiber core was imaged using a 4X objective (Olympus) focused onto a CMOS camera (FLIR Systems, Wilsonville, OR). Bonsai software[80] was used to select the fiber cores and acquire fluorescence intensity signals at each wavelength at 20 Hz. Bonsai simultaneously collected analog timestamps for lever presses, headentries, reward delivery via TTL pulses sent from MED-PC and collected using Arduino Duo microprocessors (Arduino, Somerville, MA) with custom code. Photometry and behavioral data were imported into Matlab (Mathworks Inc., Natick, MA) for analysis using custom scripts (\ls://github.com/gremellab/Hold-Down-Behavior-GCAMP-Opto-analysis. https://doi.org/10.5281/zenodo.7972046

We fit the fluorescence intensity signal to a double exponential to account for photobleaching across a session. As 405 nm can also excite GCaMP, thus it is possible to create a negative trace when subtracting isosbestic signal from 470 nm signal. The present data is analyzed without 405 nm subtraction (subtraction of 405 nm did not change our results). Of note, our data itself argues against motion artifacts, as calcium was differentially modulated during similar actions by future success of that particular lever press. To check for bad coupling of the fiber to the ferrule or low expression, each session we calculated the 97.5 percentile of DF/F and ensured that there was at least a 1% change within a 15 sec moving window; sessions failing to meet this criterion were excluded from analyses.[81] We also excluded sessions with visual anomalies in the session long traces (e.g., a sudden, sustained jump in activity that could indicate fiber decoupling). For calcium transient analyses (Figures 3B and 3C), we used Matlab's findpeaks function, with the 'MinPeakHeight' argument set to 4*median absolute deviation plus the mean of the session-long calcium signal.[63] We used the mean and standard deviation during a baseline period –15s to −5s preceding the lever press to z-score press-related activity (i.e., from −5s prior to onset up to 5s post offset). The session long mean was used to calculate %dF/F as: ((F - Fmean)/Fmean) × 100%. We bootstrapped 99% confidence intervals using the boot_CI function.[64] For examining activity during lever pressing, we used Makima interpolation with Matlab's interp1 function. To compare activity in Air and CIE mice, we either collapsed all 1600ms lever press-related activity together (thus preserving the individual variance in activity within each mouse, Figure 3D), or calculated an average trace per mouse (thus removing individual variance in activity, but ensuring that our results were not due to unequal numbers of lever press-aligned data from individual animals skewing the data, Figure 3E). For the non-averaged data, we performed running permutation tests that required at least 4 adjacent samples to significantly differ from one another.[64] For the mouse-average

data, we performed 2-way RM ANOVA. Calcium activity data was smoothed using a 10 sample (or 5 sample for interpolated activity) long Gaussian filter for display purposes only.

Chemogenetic inhibition—Animals underwent behavioral training as above. To target behavioral measurements to a time period overlapping with circuit attenuation[82] that also avoids indirect effects of agonist treatment,[83] all mice were given intraperitoneal injections of the hM4Di selective agonist Clozapine-N-Oxide (CNO, 1.0 mg/kg, 10 ml/kg, Sigma Aldrich) 30 minutes prior to each hold down training session.

Slice electrophysiology—Between 5 and 21 days post last vapor exposure, mice were deeply anesthetized with isoflurane and decapitated, after which brains were extracted and placed into a continuously bubbled (95% O_2/5% CO_2) ice-cold (4°C) NMDG cutting solution (in mM: NMDG 93; KCL 2.5; NaH_2PO_4 1.2; $NaHCO_3$ 30; HEPES 20; Glucose 25; Na-Pyruvate 3; $MgCl_2$ 10; $CaCl_2$ 0.5; made using pH-neutralized 1M NMDG stock) and sliced coronally (250 mm width) using a PELCO easiSlicer vibrating microtome (Ted Pella, Inc, Redding, CA). Slices were then incubated in warm (35°C) NMDG solution for 5 minutes, after which they were transferred to a HEPES-modified recovery solution (in mM: NaCl 112; KCl 3; NaH_2PO_4 1.2; $NaHCO_3$ 35; HEPES 20; Glucose 11; Ascorbate 0.4; $MgCl_2$ 1; $CaCl_2$ 2.5) at room temperature (23°C) for at least 45 minutes before recording. Whole-cell current clamp recordings were performed in M2-DMS projection neurons. M2-DMS projection cells were identified by the fluorescent label, using an Olympus BX51WI microscope mounted on a vibration isolation table and a high-power LED (Thorlabs, LED4D067). Recordings were made in ACSF containing (in mM): 126 NaCl, 26 NaHCO3, 1.2 NaH2PO4, 3 KCl, 1.5 MgCl2, 2.4 CaCl2, and 11 D-Glucose, continuously bubbled with 95% O_2/5% CO_2. ACSF was continuously perfused at a rate of 2.5 mL/min and maintained at a temperature of 32°C. Recording electrodes were made with borosilicate glass capillaries (Sutter Instruments, Novato California) using a PC-10 puller (Narishige International, Amityville, NY) to yield resistances between 3–6 MU. Electrodes were filled with an internal solution (in mM: 128 K-Gluconate; 7 KCl; 3 NaCl; 0.2 EGTA; 10 HEPES; 4 Mg-ATP; 0.3 Na_2-GTP; 290 mOsm; pH 7.2). Recordings were made using a MultiClamp 700B amplifier (Molecular Devices, Union City, CA), filtered at 2 kHz, digitized at 10 kHz with an Instrutech ITC-18 (HEKA Instruments, Bellmore, NY). Acquisition and stimulation was performed using WinWCP (University of Strathclyde, Glasgow, UK). For current clamp experiments, resting membrane potential (RMP) was acquired within the first 3 minutes of break-in. Input resistance (R_{in}) was calculated by generating an I/V curve using fixed current injections steps (−200 to 50pA in 50pA increments) and measuring the steady state voltage. I/F curves were generated with a series of fixed current injections (50 pA increments from 0 to 600 pA) to elicit action potential firing. Rheobase was defined as the least amount of current to drive a cell to fire and was measured by stimulating at 3pA increments. For CNO validation, a single step pulse of 300pA was used to measure cell excitability. For CNO verification, we used a concentration of 10mM CNO in recording ACSF as described above, and one cell (identified by fluorescence) per slice was recorded prior to and post CNO wash on. Cells were excluded from analysis if series resistance (R_{-s}) changed by >20% or if RMP was below −50mV. Analysis of electrophysiology data was performed using WinWCP (University of Strathclyde, Glasgow, UK) and Easy Electrophysiology.

Data analysis

Linear mixed effect models: We built Linear Mixed Effects models (LME) to model the relationship between the duration of lever press n (i.e., the current press) and n-back (n – 1 through n – 10) lever press durations. We included random intercept terms for mouse and day of training to account for the repeated structure of our data. To account for variance explained by the overall performance within a session, fixed terms included the overall percentage of rewarded lever presses as well as the timestamps of when each lever press occurred within a session. To determine if predictive relationships were contingent upon their sequential order, beta coefficient outputs pertaining to lever press duration were compared to beta coefficients obtained from 1,000 order shuffled distributions using permutation testing. Importantly, shuffling occurred within individual sessions/mice to preserve overall performance statistics (e.g. total lever presses and their durations made by that mouse in that session), and the order shuffling for each (n - x back) lever press occurred independently from each other (e.g., for comparison between actual and order shuffled n – 3, only n – 3 back was shuffled, leaving the surrounding n-x back in the same sequential order).

$$n = \beta_0 + \beta_{n-1}n_{-1} + \beta_{n-2}n_{-2} + \ldots + \beta_{n-10}n_{-10} + \beta_t(t) + \beta\%(\%) + (1|M) + (1|D) + \varepsilon_i$$

Where n is the current lever press duration, $n-1$ through $n-10$ are the previous 1 through 10 lever press durations and β_x is the linear regression coefficient for term × (β_0 is the intercept term). Additional terms include covariates of time in session (t) ,the percentage of presses that met criteria (%), and the random intercept terms for both mouse (M) and day (D). For our initial analyses, we built separate LMEs for each group (e.g., an LME for Air mice and one for CIE mice in Figure 2D). As a control, we alternatively built LMEs with data from all groups collapsed together, with indicator variables specifying which group the data came from. This allowed us to add interaction terms between, e.g., $n-1$× Group to see if the magnitude of the $n-1$ coefficient differed based on group status (Air/CIE and/or Ctl/H4).

We also sought to determine if CIE altered the relationship between prior behavior and current calcium activity. Therefore, we built LMEs to predict calcium activity before press onset (−1s to 0s), during the press, and after press offset (0s to +1s), using data from all 1,600ms training days. We used the area under the curve of the calcium activity, and tried to predict this activity using both current and prior durations, as well as prior activity to control for autocorrelation in the calcium signal.

$$A = \beta_0 + \beta_n n_0 + \beta_{n-1}n_{-1} + \ldots + \beta_{n-6}n_{-6} + \beta_{A\text{-}1}A_{-1} + \ldots + \beta_{A-6}A_{-6} + (1|M) + (1|D) + \varepsilon_i$$

Where A is current calcium activity and β_x is the regression coefficient for term x. Of note, these models included n duration (n_0) as a predictor (whereas this was what we predicted in the pure behavioral models). We predicted A given both current ($n0$) and prior ($n-1$, up to $n-6$) press durations, included prior Ca^{2+} activity ($A-1$, up to $A-6$) as a covariate, and included random intercepts of mouse (M) and training day (D).

Decoding—We used a support vector machine (SVM) classifier trained on individual mouse/sessions to predict press durations using M2-DMS calcium activity data. We created four equal sample duration bins within each individual mouse/session - thus, chance performance was 25%. Next, we used several calcium activity measurements as predictors including the area under the curve, and the slope of the calcium signal from: −1s to 0s prior to press onset, during the press, 0s to +1s after press release, and from +2s to +5s after press release. We then trained the SVM classifier using Matlab's fitcoec function, using additional arguments to standardize the calcium activity data and to specify a linear kernel function. We performed 10 k-fold cross validations on the model, subtracted the classification loss from 1, and multiplied by 100 to get the classification accuracy %.

QUANTIFICATION AND STATISTICAL ANALYSIS

All analyses were two-tailed with $\alpha = 0.05$ as a threshold for significance. Statistical results can be found in legends and in the results section. Qualitative histological exclusion of animals due to viral expression or fiber placement was blind, but subsequent quantitative data analysis was not blinded. For analyzing coarse behavioral measurements (e.g., Total Lever Presses) Repeated Measures (RM) ANOVAs were used (with Greenhouse-Geisser corrections if preliminary analyses indicated different sample standard deviations), with Bonferroni corrections for post-hoc multiple comparisons. We used Mann-Whitney tests when preliminary tests indicated non-normal distributions. In our LME models, we used permutation tests comparing actual β coefficient values to a distribution of 1000 order shuffled versions of the same variable, and thus the resolution of our permutation p-values was $p < 0.001$. We excluded anomalous presses (>16s in duration) from all datasets. For group comparisons (e.g., Air vs. CIE) of LME model coefficients, we used 2-way or 3-way ANOVA, with follow-up post hoc corrected comparisons for individual n-backs, and additionally built LME models using all groups with treatment as an indicator variable. Behavioral data was analyzed using Excel (Microsoft), Matlab (Mathworks), R (R Core Team) and the rmcorr package,[76] JASP, and Prism (Graphpad).

Supplementary Material

Refer to Web version on PubMed Central for supplementary material.

ACKNOWLEDGMENTS

This work was funded by F31AA027439 (D.C.S.), NSF-GRFP DGE-2038238 (E.T.B.), NSF-GRFP DGE-1650112 (C.C.), R01AA026077 (C.M.G.), and a Whitehall Foundation Award (C.M.G.).

REFERENCES

1. Barker JM, Bryant KG, Montiel-Ramos A, Goldwasser B, and Chandler LJ (2020). Selective deficits in contingency-driven ethanol seeking following chronic ethanol exposure in male mice. Alcohol Clin. Exp. Res 44, 1896–1905. 10.1111/acer.14418. [PubMed: 32735737]
2. Claus ED, Kiehl KA, and Hutchison KE (2011). Neural and behavioral mechanisms of impulsive choice in alcohol use disorder. Alcohol Clin. Exp. Res 35, 1209–1219. 10.1111/j.1530-0277.2011.01455.x. [PubMed: 21676001]

3. Duka T, Trick L, Nikolaou K, Gray MA, Kempton MJ, Williams H, Williams SCR, Critchley HD, and Stephens DN (2011). Unique brain areas associated with abstinence control are damaged in multiply detoxified alcoholics. Biol. Psychiatr 70, 545–552. 10.1016/j.biopsych.2011.04.006.

4. Scaife JC, and Duka T (2009). Behavioural measures of frontal lobe function in a population of young social drinkers with binge drinking pattern. Pharmacol. Biochem. Behav 93, 354–362. 10.1016/j.pbb.2009.05.015. [PubMed: 19497334]

5. Shnitko TA, Gonzales SW, Newman N, and Grant KA (2020). Behavioral Flexibility in alcohol drinking monkeys: the morning after. Alcohol Clin. Exp. Res 44, 729–737. 10.1111/acer.14289. [PubMed: 31984521]

6. Sjoerds Z, van den Brink W, Beekman ATF, Penninx BWJH, and Veltman DJ (2014). Response inhibition in alcohol-dependent patients and patients with depression/anxiety: a functional magnetic resonance imaging study. Psychol. Med 44, 1713–1725. 10.1017/S0033291713002274. [PubMed: 24016382]

7. Dickinson A (1985). Actions and habits: the development of behavioural autonomy. Philos. Trans. R. Soc. B Biol. Sci 308, 67–78. 10.1098/rstb.1985.0010.

8. Adams CD, and Dickinson A (1981). Instrumental responding following reinforcer devaluation. Q. J. Exp. Psychol. Sect. B 33, 109–121. 10.1080/14640748108400816.

9. Belin D, Belin-Rauscent A, Murray JE, and Everitt BJ (2013). Addiction: failure of control over maladaptive incentive habits. Curr. Opin. Neurobiol 23, 564–572. 10.1016/j.conb.2013.01.025. [PubMed: 23452942]

10. Everitt BJ, and Robbins TW (2005). Neural systems of reinforcement for drug addiction: from actions to habits to compulsion. Nat. Neurosci 8, 1481–1489. 10.1038/nn1579. [PubMed: 16251991]

11. Hogarth L (2020). Addiction is driven by excessive goal-directed drug choice under negative affect: translational critique of habit and compulsion theory. Neuropsychopharmacology 45, 720–735. 10.1038/s41386-020-0600-8. [PubMed: 31905368]

12. Gremel CM, and Lovinger DM (2017). Associative and sensorimotor cortico-basal ganglia circuit roles in effects of abused drugs. Genes Brain Behav 16, 71–85. 10.1111/gbb.12309. [PubMed: 27457495]

13. den Hartog C, Zamudio-Bulcock P, Nimitvilai S, Gilstrap M, Eaton B, Fedarovich H, Motts A, and Woodward JJ (2016). Inactivation of the lateral orbitofrontal cortex increases drinking in ethanol-dependent but not non-dependent mice. Neuropharmacology 107, 451–459. 10.1016/j.neuropharm.2016.03.031. [PubMed: 27016020]

14. Morningstar MD, Linsenbardt DN, and Lapish CC (2020). Ethanol alters variability, but not rate, of firing in medial prefrontal cortex neurons of awake-behaving rats. Alcohol Clin. Exp. Res 44, 2225–2238. 10.1111/acer.14463. [PubMed: 32966634]

15. Nimitvilai S, Lopez MF, Mulholland PJ, and Woodward JJ (2016). Chronic intermittent ethanol exposure enhances the excitability and synaptic plasticity of lateral orbitofrontal cortex neurons and induces a tolerance to the acute inhibitory actions of ethanol. Neuropsychopharmacology 41, 1112–1127. 10.1038/npp.2015.250. [PubMed: 26286839]

16. Nimitvilai S, Uys JD, Woodward JJ, Randall PK, Ball LE, Williams RW, Jones BC, Lu L, Grant KA, and Mulholland PJ (2017). Orbitofrontal neuroadaptations and cross-species synaptic biomarkers in heavy-drinking macaques. J. Neurosci 37, 3646–3660. 10.1523/JNEUROSCI.0133-17.2017. [PubMed: 28270566]

17. Renteria R, Baltz ET, and Gremel CM (2018). Chronic alcohol exposure disrupts top-down control over basal ganglia action selection to produce habits. Nat. Commun 9, 211. 10.1038/s41467-017-02615-9. [PubMed: 29335427]

18. Renteria R, Cazares C, Baltz ET, Schreiner DC, Yalcinbas EA, Steinkellner T, Hnasko TS, and Gremel CM (2021). Mechanism for differential recruitment of orbitostriatal transmission during actions and outcomes following chronic alcohol exposure. Elife 10, e67065. 10.7554/eLife.67065. [PubMed: 33729155]

19. Cuzon Carlson VC, Seabold GK, Helms CM, Garg N, Odagiri M, Rau AR, Daunais J, Alvarez VA, Lovinger DM, and Grant KA (2011). Synaptic and morphological neuroadaptations in the putamen

associated with long-term, relapsing alcohol drinking in primates. Neuropsychopharmacology 36, 2513–2528. [PubMed: 21796110]

20. Cuzon Carlson VC (2018). GABA and glutamate synaptic coadaptations to chronic ethanol in the striatum. In The Neuropharmacology of Alcohol Handbook of Experimental Pharmacology, Grant KA and Lovinger DM, eds. (Springer International Publishing), pp. 79–112. 10.1007/164_2018_98.
21. Lovinger DM, and Alvarez VA (2017). Alcohol and basal ganglia circuitry: Animal models. Neuropharmacology 122, 46–55. 10.1016/j.neuropharm.2017.03.023. [PubMed: 28341206]
22. Ma T, Cheng Y, Roltsch Hellard E, Wang X, Lu J, Gao X, Huang CCY, Wei X-Y, Ji J-Y, and Wang J (2018). Bidirectional and long-lasting control of alcohol-seeking behavior by corticostriatal LTP and LTD. Nat. Neurosci 21, 373–383. 10.1038/s41593-018-0081-9. [PubMed: 29434375]
23. Muñoz B, Fritz BM, Yin F, and Atwood BK (2018). Alcohol exposure disrupts mu opioid receptor-mediated long-term depression at insular cortex inputs to dorsolateral striatum. Nat. Commun 9, 1318. 10.1038/s41467-018-03683-1. [PubMed: 29615610]
24. Patton MS, Heckman M, Kim C, Mu C, and Mathur BN (2021). Compulsive alcohol consumption is regulated by dorsal striatum fast-spiking interneurons. Neuropsychopharmacology 46, 351–359. 10.1038/s41386-020-0766-0. [PubMed: 32663841]
25. Morris LS, Baek K, Tait R, Elliott R, Ersche KD, Flechais R, McGonigle J, Murphy A, Nestor LJ, Orban C, et al. (2018). Naltrexone ameliorates functional network abnormalities in alcohol-dependent individuals. Addiction Biol 23, 425–436. 10.1111/adb.12503.
26. Aron AR (2011). From reactive to proactive and selective control: developing a richer model for stopping inappropriate responses. Biol. Psychiatr 69, e55–e68. 10.1016/j.biopsych.2010.07.024.
27. Aron AR, Behrens TE, Smith S, Frank MJ, and Poldrack RA (2007). Triangulating a cognitive control network using diffusion-weighted magnetic resonance imaging (MRI) and functional MRI. J. Neurosci 27, 3743–3752. 10.1523/JNEUROSCI.0519-07.2007. [PubMed: 17409238]
28. Morris LS, Kundu P, Dowell N, Mechelmans DJ, Favre P, Irvine MA, Robbins TW, Daw N, Bullmore ET, Harrison NA, and Voon V (2016). Fronto-striatal organization: defining functional and microstructural substrates of behavioural flexibility. Cortex 74, 118–133. 10.1016/j.cortex.2015.11.004. [PubMed: 26673945]
29. Isoda M, and Hikosaka O (2007). Switching from automatic to controlled action by monkey medial frontal cortex. Nat. Neurosci 10, 240–248. 10.1038/nn1830. [PubMed: 17237780]
30. Gomes PVO, Brasil-Neto JP, Allam N, and Rodrigues de Souza E (2012). A randomized, double-blind trial of repetitive transcranial magnetic stimulation in obsessive-compulsive disorder with three-month follow-up. J. Neuropsychiatry Clin. Neurosci 24, 437–443. 10.1176/appi.neuropsych.11100242. [PubMed: 23224449]
31. Hawken ER, Dilkov D, Kaludiev E, Simek S, Zhang F, and Milev R (2016). Transcranial magnetic stimulation of the supplementary motor area in the treatment of obsessive-compulsive disorder: a multi-site study. Int. J. Mol. Sci 17, 420. 10.3390/ijms17030420. [PubMed: 27011177]
32. Mantovani A, Rossi S, Bassi BD, Simpson HB, Fallon BA, and Lisanby SH (2013). Modulation of motor cortex excitability in obsessive-compulsive disorder: an exploratory study on the relations of neurophysiology measures with clinical outcome. Psychiatr. Res 210, 1026–1032. 10.1016/j.psychres.2013.08.054.
33. Barthas F, and Kwan AC (2017). Secondary motor cortex: where ‘sensory’ meets ‘motor’ in the rodent frontal cortex. Trends Neurosci 40, 181–193. 10.1016/j.tins.2016.11.006. [PubMed: 28012708]
34. Gremel CM, and Costa RM (2013). Premotor cortex is critical for goal-directed actions. Front. Comput. Neurosci 7, 110. 10.3389/fncom.2013.00110. [PubMed: 23964233]
35. Hattori R, Danskin B, Babic Z, Mlynaryk N, and Komiyama T (2019). Area-specificity and plasticity of history-dependent value coding during learning. Cell 177, 1858–1872.e15. 10.1016/j.cell.2019.04.027. [PubMed: 31080067]
36. Murakami M, Vicente MI, Costa GM, and Mainen ZF (2014). Neural antecedents of self-initiated actions in secondary motor cortex. Nat. Neurosci 17, 1574–1582. 10.1038/nn.3826. [PubMed: 25262496]

37. Murakami M, Shteingart H, Loewenstein Y, and Mainen ZF (2017). Distinct sources of deterministic and stochastic components of action timing decisions in rodent frontal cortex. Neuron 94, 908–919.e7. 10.1016/j.neuron.2017.04.040. [PubMed: 28521140]
38. Siniscalchi MJ, Phoumthipphavong V, Ali F, Lozano M, and Kwan AC (2016). Fast and slow transitions in frontal ensemble activity during flexible sensorimotor behavior. Nat. Neurosci 19, 1234–1242. 10.1038/nn.4342. [PubMed: 27399844]
39. Sul JH, Jo S, Lee D, and Jung MW (2011). Role of rodent secondary motor cortex in value-based action selection. Nat. Neurosci 14, 1202–1208. 10.1038/nn.2881. [PubMed: 21841777]
40. Schreiner DC, Cazares C, Renteria R, and Gremel CM (2022). Information normally considered task-irrelevant drives decision-making and affects premotor circuit recruitment. Nat. Commun 13, 2134. 10.1038/s41467-022-29807-2. [PubMed: 35440120]
41. Schreiner DC, and Gremel CM (2018). Orbital frontal cortex projections to secondary motor cortex mediate exploitation of learned rules. Sci. Rep 8, 10979. 10.1038/s41598-018-29285-x. [PubMed: 30030509]
42. Delevich K, Okada NJ, Rahane A, Zhang Z, Hall CD, and Wilbrecht L (2020). Sex and pubertal status influence dendritic spine density on frontal corticostriatal projection neurons in mice. Cerebr. Cortex 30, 3543–3557. 10.1093/cercor/bhz325.
43. Hintiryan H, Foster NN, Bowman I, Bay M, Song MY, Gou L, Yamashita S, Bienkowski MS, Zingg B, Zhu M, et al. (2016). The mouse cortico-striatal projectome. Nat. Neurosci 19, 1100–1114. 10.1038/nn.4332. [PubMed: 27322419]
44. Hunnicutt BJ, Jongbloets BC, Birdsong WT, Gertz KJ, Zhong H, and Mao T (2016). A comprehensive excitatory input map of the striatum reveals novel functional organization. Elife 5, e19103. 10.7554/eLife.19103. [PubMed: 27892854]
45. Magno LAV, Tenza-Ferrer H, Collodetti M, Aguiar MFG, Rodrigues APC, da Silva RS, Birbrair A, et al. (2019). Optogenetic stimulation of the M2 cortex reverts motor dysfunction in a mouse model of Parkinson's Disease. J. Neurosci 39, 3234–3248. 10.1523/JNEURO-SCI.2277-18.2019. [PubMed: 30782975]
46. Corbit VL, Manning EE, Gittis AH, and Ahmari SE (2019). Strengthened inputs from secondary motor cortex to striatum in a mouse model of compulsive behavior. J. Neurosci 39, 2965–2975. 10.1523/JNEUROSCI.1728-18.2018. [PubMed: 30737313]
47. Liu W, and Crews FT (2015). Adolescent Intermittent ethanol exposure enhances ethanol activation of the nucleus accumbens while blunting the prefrontal cortex responses in adult rat. Neuroscience 293, 92–108. 10.1016/j.neuroscience.2015.02.014. [PubMed: 25727639]
48. Dudek M, Abo-Ramadan U, Hermann D, Brown M, Canals S, Sommer WH, and Hyytiä P (2015). Brain activation induced by voluntary alcohol and saccharin drinking in rats assessed with manganese-enhanced magnetic resonance imaging. Addiction Biol 20, 1012–1021. 10.1111/adb.12179.
49. Becker HC, and Hale RL (1993). Repeated episodes of ethanol withdrawal potentiate the severity of subsequent withdrawal seizures: an animal model of alcohol withdrawal 'kindling.'. Alcohol Clin. Exp. Res 17, 94–98. 10.1111/j.1530-0277.1993.tb00731.x. [PubMed: 8452212]
50. Becker HC, and Lopez MF (2004). Increased ethanol drinking after repeated chronic ethanol exposure and withdrawal experience in C57BL/6 mice. Alcohol Clin. Exp. Res 28, 1829–1838. 10.1097/01.ALC.0000149977.95306.3A. [PubMed: 15608599]
51. Becker HC, and Lopez MF (2004). Increased ethanol drinking after repeated chronic ethanol exposure and withdrawal experience in C57BL/6 mice. Alcohol Clin. Exp. Res 28, 1829–1838. 10.1097/01.ALC.0000149977.95306.3A. [PubMed: 15608599]
52. Cazares C, Schreiner DC, and Gremel CM (2021). Different effects of alcohol exposure on action and outcome related orbitofrontal cortex activity. eNeuro 8, ENEURO.0052, 21.2021. 10.1523/ENEURO.0052-21.2021.
53. Lopez MF, and Becker HC (2005). Effect of pattern and number of chronic ethanol exposures on subsequent voluntary ethanol intake in C57BL/6J mice. Psychopharmacology (Berl.) 181, 688–696. 10.1007/s00213-005-0026-3. [PubMed: 16001125]

54. Renteria R, Cazares C, and Gremel CM (2020). Habitual ethanol seeking and licking microstructure of enhanced ethanol self-administration in ethanol-dependent mice. Alcohol Clin. Exp. Res 44, 880–891. [PubMed: 32020644]
55. Heilig M, Egli M, Crabbe JC, and Becker HC (2010). Acute withdrawal, protracted abstinence and negative affect in alcoholism: are they linked? Addict. Biol 15, 169–184. 10.1111/j.1369-1600.2009.00194.x. [PubMed: 20148778]
56. Fan D, Rossi MA, and Yin HH (2012). Mechanisms of action selection and timing in substantia nigra neurons. J. Neurosci 32, 5534–5548. 10.1523/JNEUROSCI.5924-11.2012. [PubMed: 22514315]
57. Platt JR, Kuch DO, and Bitgood SC (1973). Rats' lever-press durations as psychophysical judgments of time. J. Exp. Anal. Behav 19, 239–250. 10.1901/jeab.1973.19-239. [PubMed: 4716170]
58. Cazares C, Schreiner DC, Valencia ML, and Gremel CM (2022). Orbitofrontal cortex populations are differentially recruited to support actions. Curr. Biol 32, 4675–4687.e5. 10.1016/j.cub.2022.09.022. [PubMed: 36195096]
59. Yin HH (2009). The role of the murine motor cortex in action duration and order. Front. Integr. Neurosci 3, 23. 10.3389/neuro.07.023.2009. [PubMed: 19847323]
60. Schreiner DC, Yalcinbas EA, and Gremel CM (2021). A push for examining subjective experience in value-based decision-making. Curr. Opin. Behav. Sci 41, 45–49. 10.1016/j.cobeha.2021.03.020. [PubMed: 34056054]
61. Schreiner DC, Renteria R, and Gremel CM (2020). Fractionating the all-or-nothing definition of goal-directed and habitual decision-making. J. Neurosci. Res 98, 998–1006. 10.1002/jnr.24545. [PubMed: 31642551]
62. Morris LS, Baek K, Kundu P, Harrison NA, Frank MJ, and Voon V (2016). Biases in the explore–exploit tradeoff in addictions: the role of avoidance of uncertainty. Neuropsychopharmacology 41, 940–948. 10.1038/npp.2015.208. [PubMed: 26174598]
63. Pribiag H, Shin S, Wang EH-J, Sun F, Datta P, Okamoto A, Guss H, Jain A, Wang X-Y, De Freitas B, et al. (2021). Ventral pallidum DRD3 potentiates a pallido-habenular circuit driving accumbal dopamine release and cocaine seeking. Neuron 109, 2165–2182.e10. 10.1016/j.neuron.2021.05.002. [PubMed: 34048697]
64. Jean-Richard-dit-Bressel P, Clifford CWG, and McNally GP (2020). Analyzing event-related transients: confidence intervals, permutation tests, and consecutive thresholds. Front. Mol. Neurosci 13, 14. 10.3389/fnmol.2020.00014. [PubMed: 32116547]
65. McCalley DM, Kaur N, Wolf JP, Contreras IE, Book SW, Smith JP, and Hanlon CA (2023). Medial prefrontal cortex theta burst stimulation improves treatment outcomes in Alcohol Use Disorder: a double-blind, sham-controlled neuroimaging study. Biol. Psychiatry Glob. Open Sci 3, 301–310. 10.1016/j.bpsgos.2022.03.002. [PubMed: 37124360]
66. Barker JM, Corbit LH, Robinson DL, Gremel CM, Gonzales RA, and Chandler LJ (2015). Corticostriatal circuitry and habitual ethanol seeking. Alcohol 49, 817–824. 10.1016/j.alcohol.2015.03.003. [PubMed: 26059221]
67. Corbit LH, and Janak PH (2016). Habitual alcohol seeking: neural bases and possible relations to alcohol use disorders. Alcohol Clin. Exp. Res 40, 1380–1389. 10.1111/acer.13094. [PubMed: 27223341]
68. Dickinson A, Wood N, and Smith JW (2002). Alcohol seeking by rats: action or habit? Q. J. Exp. Psychol. B 55, 331–348. 10.1080/0272499024400016. [PubMed: 12350285]
69. Sjoerds Z, de Wit S, van den Brink W, Robbins TW, Beekman ATF, Penninx BWJH, and Veltman DJ (2013). Behavioral and neuroimaging evidence for overreliance on habit learning in alcohol-dependent patients. Transl. Psychiatry 3, e337. 10.1038/tp.2013.107. [PubMed: 24346135]
70. Lovinger DM, and Gremel CM (2021). A circuit-based information approach to substance abuse research. Trends Neurosci 44, 122–135. 10.1016/j.tins.2020.10.005. [PubMed: 33168235]
71. Tecuapetla F, Jin X, Lima SQ, and Costa RM (2016). Complementary contributions of striatal projection pathways to action initiation and execution. Cell 166, 703–715. 10.1016/j.cell.2016.06.032. [PubMed: 27453468]

72. Moorman DE (2018). The role of the orbitofrontal cortex in alcohol use, abuse, and dependence. Prog. Neuro-Psychopharmacol. Biol. Psychiatry 87, 85–107. 10.1016/j.pnpbp.2018.01.010.

73. Shields CN, and Gremel CM (2020). Review of orbitofrontal cortex in alcohol dependence: a disrupted cognitive map? Alcohol. Clin. Exp. Res 44, 1952–1964. 10.1111/acer.14441. [PubMed: 32852095]

74. Johnson CM, Peckler H, Tai L-H, and Wilbrecht L (2016). Rule learning enhances structural plasticity of long-range axons in frontal cortex. Nat. Commun 7, 10785. 10.1038/ncomms10785. [PubMed: 26949122]

75. Rothwell PE, Hayton SJ, Sun GL, Fuccillo MV, Lim BK, and Malenka RC (2015). Input- and output-specific regulation of serial order performance by corticostriatal circuits. Neuron 88, 345–356. 10.1016/j.neuron.2015.09.035. [PubMed: 26494279]

76. Bakdash JZ, and Marusich LR (2017). Repeated measures correlation. Front. Psychol 8, 456. 10.3389/fpsyg.2017.00456. [PubMed: 28439244]

77. Rothermel M, Brunert D, Zabawa C, Díaz-Quesada M, and Wachowiak M (2013). Transgene expression in target-defined neuron populations mediated by retrograde infection with adeno-associated viral vectors. J. Neurosci 33, 15195–15206. 10.1523/JNEUROSCI.1618-13.2013. [PubMed: 24048849]

78. Dias-Ferreira E, Sousa JC, Melo I, Morgado P, Mesquita AR, Cerqueira JJ, Costa RM, and Sousa N (2009). Chronic stress causes Frontostriatal reorganization and affects decision-making. Science 325, 621–625. 10.1126/science.1171203. [PubMed: 19644122]

79. Pereira EF, Aracava Y, Aronstam RS, Barreiro EJ, and Albuquerque EX (1992). Pyrazole, an alcohol dehydrogenase inhibitor, has dual effects on N-methyl-D-aspartate receptors of hippocampal pyramidal cells: agonist and noncompetitive antagonist. J. Pharmacol. Exp. Therapeut 261, 331–340.

80. Lopes G, Bonacchi N, Frazão J, Neto JP, Atallah BV, Soares S, Moreira L, Matias S, Itskov PM, Correia PA, et al. (2015). Bonsai: an event-based framework for processing and controlling data streams. Front. Neuroinf 9, 7. 10.3389/fninf.2015.00007.

81. Markowitz JE, Gillis WF, Beron CC, Neufeld SQ, Robertson K, Bhagat ND, Peterson RE, Peterson E, Hyun M, Linderman SW, et al. (2018). The striatum organizes 3D behavior via moment-to-moment action selection. Cell 174, 44–58.e17. 10.1016/j.cell.2018.04.019. [PubMed: 29779950]

82. Gremel CM, and Costa RM (2013). Orbitofrontal and striatal circuits dynamically encode the shift between goal-directed and habitual actions. Nat. Commun 4, 2264. 10.1038/ncomms3264. [PubMed: 23921250]

83. Gomez JL, Bonaventura J, Lesniak W, Mathews WB, Sysa-Shah P, Rodriguez LA, Ellis RJ, Richie CT, Harvey BK, Dannals RF, et al. (2017). Chemogenetics revealed: DREADD occupancy and activation via converted clozapine. Science 357, 503–507. 10.1126/science.aan2475. [PubMed: 28774929]

Highlights

- Chronic alcohol disrupts action control
- Chronic alcohol induces hyperactive M2-DMS during action control
- Chemogenetic suppression of M2-DMS hyperactivity rescues action control

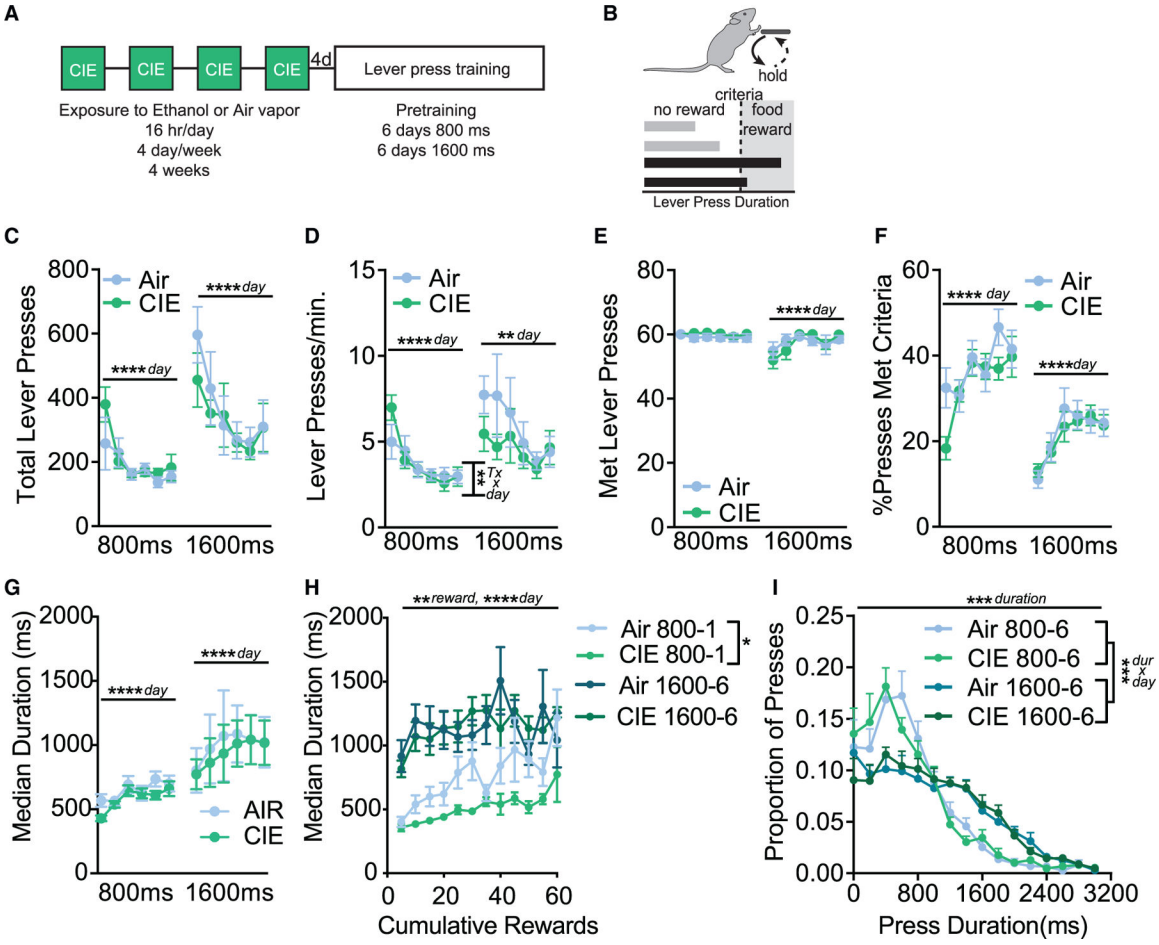

Figure 1. Both Air and CIE mice learn a self-generated, self-paced lever hold-down task

(A) CIE (chronic intermittent ethanol) vapor exposure timeline.

(B) Hold-down task schematic: mice had to press and hold down the lever for at least a minimum duration to earn food reward, without trials or cues, with reward delivered immediately after press release.

(C) Mean number of total lever presses across days for all mice (n = 8 Air, n = 8 CIE). 800 ms indicates days with a duration criterion of >800 ms, while 1,600 ms indicates days with a criterion of >1,600 ms. There was a main effect of day of training during both 800 (two-way repeated measures [RM] ANOVA, (day × group): $F_{5,70} = 6.94$, $p < 0.0010$) and 1,600 ms criterion training ($F_{5,70} = 9.45$, $p < 0.0001$) but no group differences, nor an interaction.

(D) There was a main effect of day on rate of lever pressing for 800 ms training ($F_{5,70} = 21$, $p < 0.0001$), and a day × treatment interaction ($F_{5,70} = 3.07$, $p = 0.015$). No individual days differed in post hoc testing. For 1,600 ms training, there was only a main effect of day during 1,600 ms training on the lever press rate ($F_{5,70} = 4.03$, $p = 0.0028$).

(E) Average number of met lever presses (i.e., rewarded presses) across days. Main effect only of day, only during 1,600 ms training ($F_{5,70} = 5.92$, $p = 0.0001$).

(F) The percentage of lever presses that met criteria across days. Main effects only of day during both the 800 ($F_{5,70} = 8.12$, $p < 0.0001$) and 1,600 ms trainings ($F_{5,70} = 18.7$, $p < 0.0001$).

(G) Median duration of lever presses across days. A two-way RM ANOVA (day × group) revealed a main effect only of day for 800 and 1,600 ms duration criteria (all $F_{5,70} > 6.07$, all $p < 0.0001$).

(H) Median duration within a single training session, grouped by cumulative number of rewards. A three-way RM ANOVA (reward bin × group × criterion) revealed a two-way group × criterion interaction ($F_{11,153} = 12.48$, $p = 0.0005$) and main effects of reward bin, group, and duration (all $F > 3.075$, all $p < 0.0015$). Post hoc analysis showed a main effect of group at 800 ms ($F_{1,14} = 10.31$, $p < 0.01$).

(I) The distribution of lever press durations on the final (i.e., the sixth) 800 and final 1,600 ms training days. A three-way RM ANOVA (duration bin × group × criterion) revealed a main effect only of duration bin ($F_{15,420} = 74.6$, $p < 0.001$) and a duration bin × criterion (day) interaction ($F_{15,420} = 9.17$, $p < 0.001$). Data points represent mean ± SEM. *$p < 0.05$, **$p < 0.01$, ***$p < 0.001$, ****$p < 0.0001$.

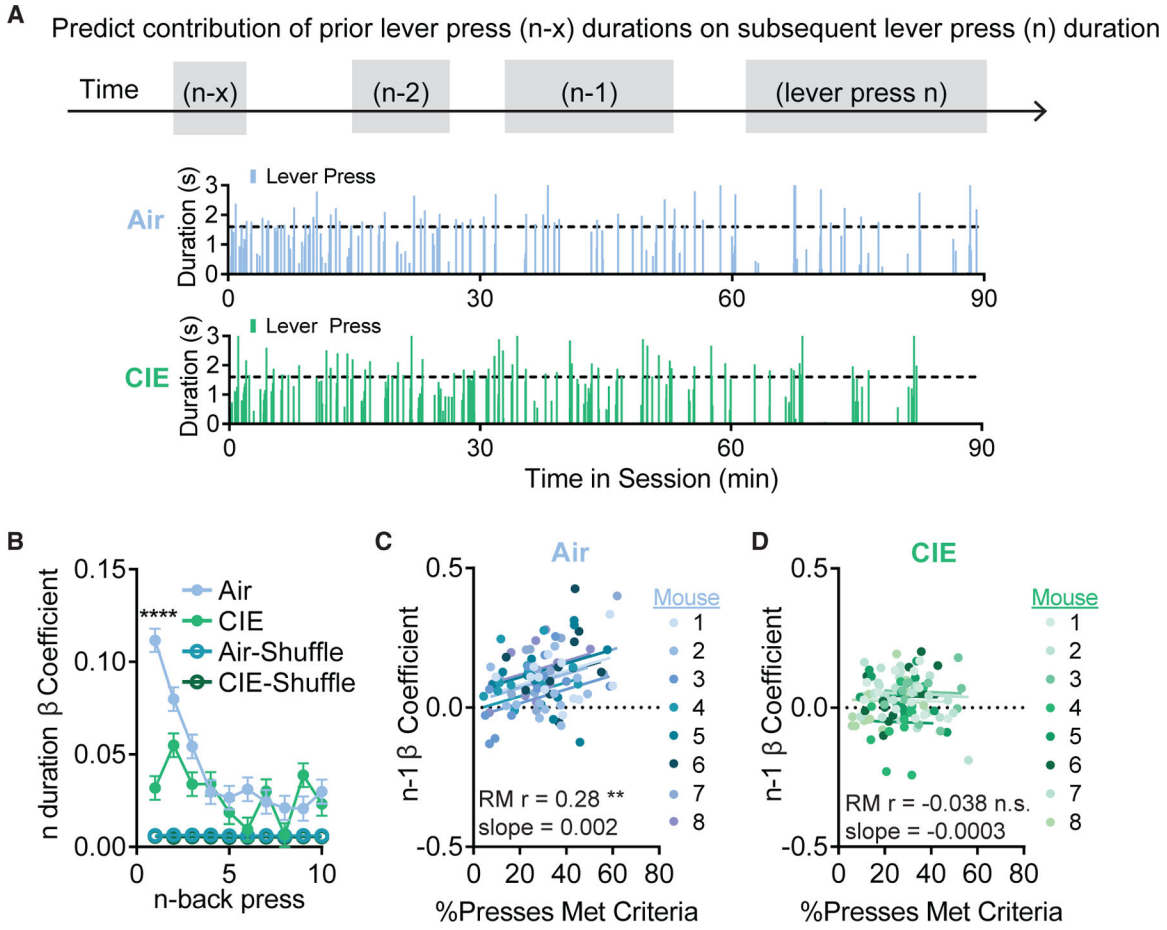

Figure 2. Prior CIE decreases the use of recent action information

(A) We created a linear mixed effect model predicting the duration of the current lever press (n) given the durations of prior lever presses (n-back). Bottom shows representative lever press behavior for an individual session for an Air and a CIE mouse.

(B) Beta (β) coefficients for the individual n-back presses for actual and order shuffled data. A two-way ANOVA conducted on the actual data (n-back × Air/CIE Group) revealed main effects of both n-back ($F_{9,500960}$ = 18.6, p < 0.0001) and Group ($F_{1,500960}$ = 26.4, p < 0.0001), and an interaction ($F_{9,500960}$ = 8.56, p < 0.0001). Bonferroni-corrected post-hoc tests found a significant Group difference only for press n – 1 (t_{500960} = 8.76, p < 0.0001). Both Air and CIE groups significantly differed from order shuffled data (two-way ANOVA (n-back × Actual/Shuffle). Air: main effect only of Actual/Shuffle $F_{1,263480}$ = 12.8, p = 0.0003. CIE: main effect only of Actual/Shuffle $F_{1,257460}$ = 5.09, p = 0.024.

(C) β coefficients for linear mixed effect models built using individual session data and correlated with the percentage of presses that met criteria in Air mice. Shades show individual subject data across days. An RM correlation revealed a significant relationship (RM r = 0.285, DF = 87, slope = 0.002, p = 0.0069).

(D) As in (C) except for CIE mice, where there was no significant relationship between β and percentage of presses met criteria (RM correlation, RM r = −0.038, DF = 87, slope = −0.0003, p = 0.72).

Data points represent mean ± SEM. n.s., not significant. **p < 0.01, ****p < 0.0001.

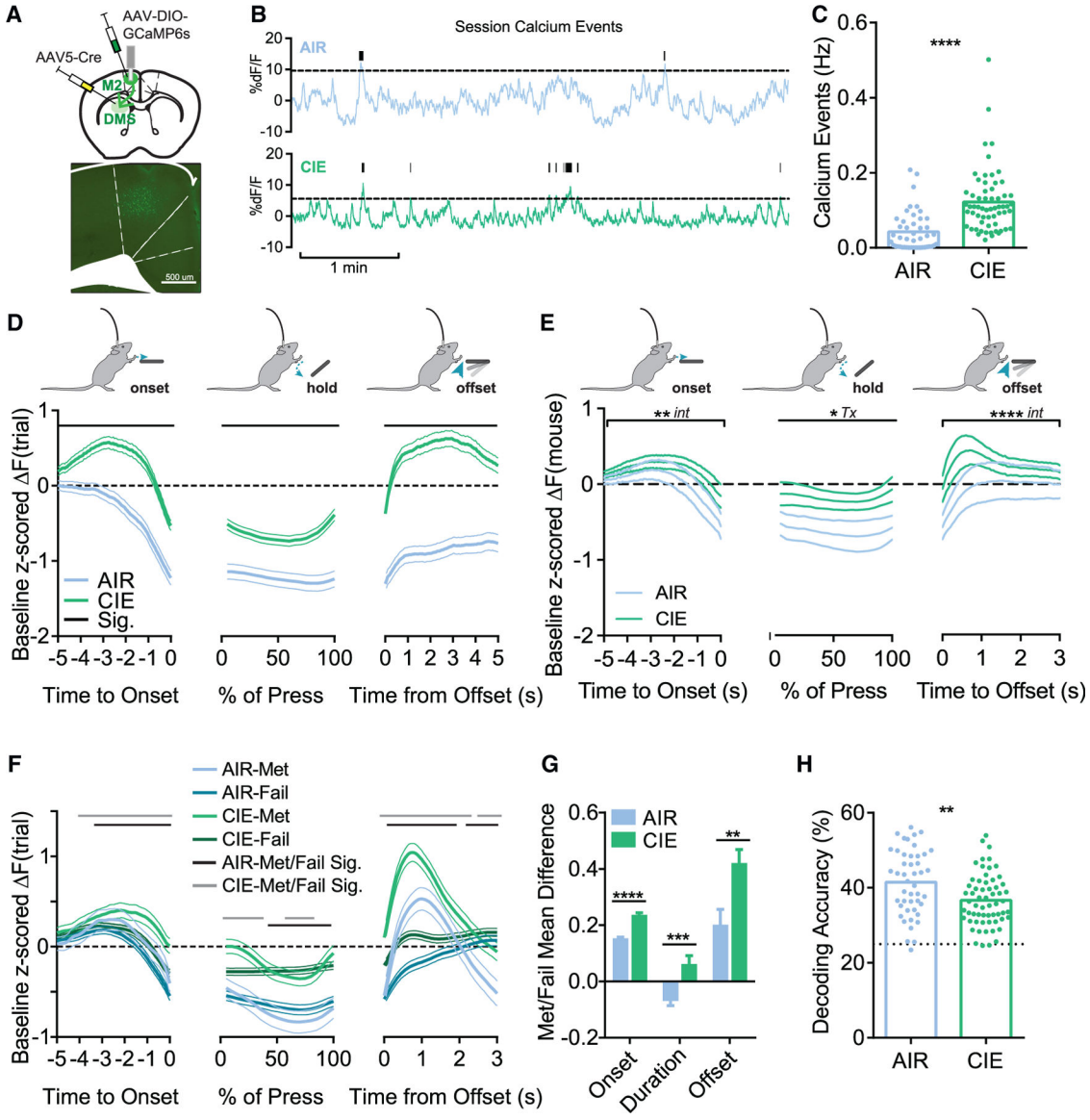

Figure 3. Prior CIE induces hyperactive calcium activity of M2-DMS projection neurons and uncouples activity and behavior

(A) (Top) Schematic of dual-virus targeting of GCaMP6s and ferrule placement to M2-DMS projection neurons to n = 6 Air and n = 8 CIE-exposed mice, and (bottom) representative fluorescent image.

(B) Representative calcium activity traces showing calcium transient analysis. Calcium signals above the dashed line were subjected to peak analysis and are indicated with tick marks above.

(C) Average calcium events (in Hz) across a session in Air and CIE mice. There was a significantly increased rate of events in CIE mice (Mann-Whitney test, U = 449, Air n = 46, CIE n = 61, $p < 0.0001$).

(D) Calcium activity z scored to a baseline period (−15 to −5 s prior to press onset) aligned to the onset (left), time-warped hold duration (middle), and offset (right) of a lever press

(lever presses n = 11,200 Air, n = 14,792 CIE). Black bars indicate time points for which there is a significant Air/CIE difference (Sig.), determined via permutation tests.
(E) As in (D) except showing data from averages per mouse (Air n = 6, CIE n = 8). Two-way RM ANOVAs (Air/CIE group × time point) reveal at onset a main effect of time point ($F_{100,1200} = 15.2$, $p < 0.0001$) and an interaction ($F_{100,1200} = 1.56$, $p = 0.0006$), during lever pressing a main effect only of group ($F_{19,228} = 1.41$, $p = 0.046$), and at offset a main effect of time point ($F_{60,720} = 4.07$, $p < 0.0001$) and an interaction ($F_{60,720} = 2.41$, $p < 0.0001$).
(F) As in (D) except segmenting out lever presses based on whether they met the criterion (met) or failed to do so (fail) in trials from Air and CIE mice. Here, significance markers indicate permutation tests comparing met versus fail activity within Air (Air-met/fail Sig.) and within CIE (CIE-met/fail Sig.) mice.
(G) The mean difference (met – fail) in the met/fail traces from (F). Air and CIE mice differed from one another (i.e., CIE mice showed larger met/fail differences) at all three event windows (Mann-Whitney tests, onset: U = 447, Air/CIE n = 61, $p < 0.0001$; duration: U = 72, Air/CIE n = 20, $p = 0.0003$; offset: U = 1,303, Air/CIE n = 61, $p = 0.0041$).
(H) Decoding accuracy using calcium activity to predict press duration quartile. Data points are accuracy from individual sessions, and dotted line indicates chance performance (25%). Air and CIE mice significantly differed in decoding accuracy (unpaired t test, $t_{105} = 3.19$, $p = 0.0019$).
Bars in (C) and (H) show mean, (E) and (G) represent mean ± SEM, while data in (D) and (F) are mean ± 99% bootstrapped confidence intervals. Sig., significant difference. *$p < 0.05$, **$p < 0.01$, ***$p < 0.001$, ****$p < 0.0001$.
See also Figures S1 and S2.

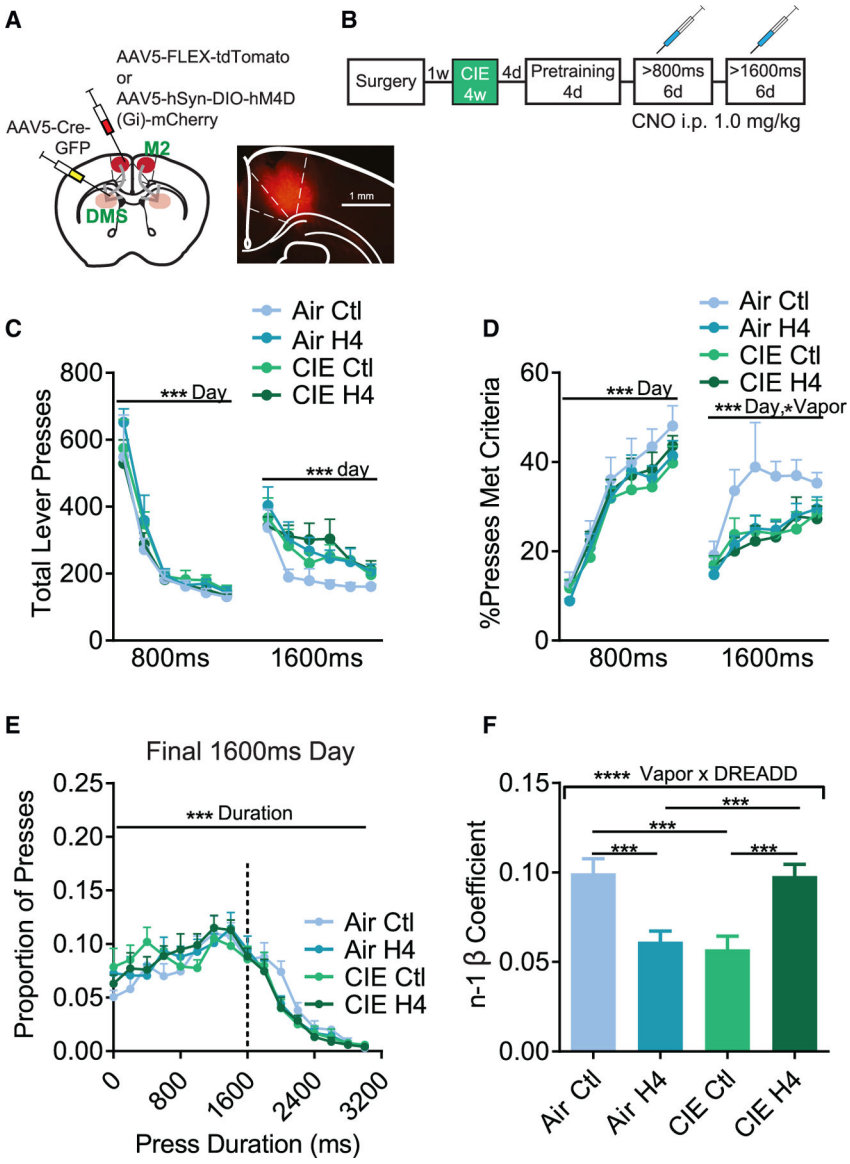

Figure 4. Chemogenetic inhibition of hyperactive M2-DMS rescues use of action information

(A) Schematic of injections and ferrule placement for chemogenetic inhibition of M2-projection neurons (left) and representative spread (right).

(B) Timeline of experiments. 1 week after surgery, mice underwent 4 rounds of vapor exposure. 4 days after the final vapor exposure, mice began pretraining, followed by criteria training of durations >800 ms for 6 days, then durations >1,600 ms for 6 days. All mice were given intraperitoneal (i.p.) injections of the H4-agonist clozapine-N-oxide (CNO; 1 mg/kg) 30 min prior to the start of each criteria session.

(C) Mean total lever presses across days of training (Air Ctl n = 6, Air H4 n = 8, CIE Ctl n = 6, CIE H4 n = 7). Main effect only of day (three-way RM ANOVA, vapor group × DREADD group × day) during both 800 ms training ($F_{5,115} = 73.4$, $p < 0.001$) and 1,600 ms days ($F_{5,115} = 22.8$, $p < 0.001$).

(D) Average percentage of presses that met criteria across days of training. Three-way RM ANOVA (vapor group × DREADD group × day) during 800 ms training showed a main effect only of day ($F_{5,115} = 99.2$, $p < 0.001$). During the 1,600 ms training, there was a main effect of day ($F_{5,115} = 14.0$, $p < 0.001$), as well as vapor group ($F_{1,23} = 4.33$, $p = 0.049$), but no main effect of DREADD group, nor interactions between factors.

(E) Distribution of lever press durations on the final day of 1,600 ms training, with a three-way RM ANOVA (vapor group × DREADD group × duration bin) showing a main effect only of duration bin ($F_{15,345} = 43.2$, $p < 0.001$). Dashed line indicates the 1,600 ms criterion.

(F) Magnitude of the n – 1 β coefficient from a linear mixed effect model using n-back durations to predict n press duration. A two-way ANOVA (vapor group × DREADD group) found no main effects but did find a significant interaction ($F_{1,85311} = 31.2$, $p < 0.0001$). Bonferroni-corrected post hoc testing revealed that there were significant differences between Air Ctl and CIE Ctl ($t_{85311} = 3.85$, $p = 0.0007$), Air Ctl and Air H4 ($t_{85311} = 3.77$, $p = 0.0010$), CIE Ctl and CIE H4 ($t_{85311} = 4.14$, $p = 0.0002$), and Air H4 and CIE H4 ($t_{85311} = 4.13$, $p = 0.0002$). Ctl, control; H4, hM4Di.

Data are mean ± SEM. *$p < 0.05$, ***$p < 0.001$, ****$p < 0.0001$. See also Figure S3.

KEY RESOURCES TABLE

REAGENT or RESOURCE	SOURCE	IDENTIFIER
Bacterial and virus strains		
pAAV.CAG.FLEX.GCaMP6s.WPRE.SV40	Addgene	100842
AAV5/Ef1a-Cre-WPRE	UNC Vector Core	N/A
rAAV5/hSyn-GFP-Cre	UNC Vector Core	N/A
rAAV5/Flex-tdTomato	UNC Vector Core	N/A
pAAV5-hSyn-DIO-hM4D(Gi)-mCherry	UNC Vector Core	N/A
rAAV5/hSyn-GFP	UNC Vector Core	N/A
rAAV5/hSyn-eYFP	UNC Vector Core	N/A
Chemicals, peptides, and recombinant proteins		
Clozapine-N-Oxide	Sigma-Aldrich	C0832
Experimental models: Organisms/strains		
C57BL/6J	The Jackson Laboratory	JAX: 000664
Software and algorithms		
Custom Analysis Code	This paper	http://github.com/gremellab/Hold-Down-Behavior-GCAMP-Opto-analysis https://doi.org/10.5281/Zenodo.7972046
RMcorr	Bakdash and Marusich[76]	https://doi.org/10.3389/fpsyg.2017.00456
GCaMP permutation testing	Jean-Richard-dit-Bressel et al.[64]	https://doi.org/10.3389/fnmol.2020.00014